

Copyright © 1981, by the author(s).
All rights reserved.

Permission to make digital or hard copies of all or part of this work for personal or classroom use is granted without fee provided that copies are not made or distributed for profit or commercial advantage and that copies bear this notice and the full citation on the first page. To copy otherwise, to republish, to post on servers or to redistribute to lists, requires prior specific permission.

ROTATIONAL INSTABILITIES IN THE FIELD-REVERSED
THETA PINCH: RESULTS OF HYBRID SIMULATIONS

by

Douglas S. Harned

Memorandum No. UCB/ERL M81/70

14 September 1981

ELECTRONICS RESEARCH LABORATORY
College of Engineering
University of California, Berkeley
94720

Rotational Instabilities in the Field-Reversed Theta Pinch:

Results of Hybrid Simulations

Douglas S. Harned

Electronics Research Laboratory

University of California

Berkeley, CA 94720

ABSTRACT

Rotational instabilities in rigidly rotating field-reversed theta pinch equilibria are studied using a quasineutral hybrid simulation code. We observe unstable $m=2$ modes at levels of ion rotation below instability thresholds predicted by finite Larmor radius fluid theory. Nonlinear effects are found to reduce the growth rate and lower the real frequency of the $m=2$ mode at large amplitude. Instabilities with $m>2$ have been observed for some strongly reversed cases. It is also found that growth rates for these instabilities can be greatly reduced by increasing the ratio of the plasma radius to the ion Larmor radius.

I. INTRODUCTION

Compact toroids have long been thought to offer promise as potential fusion reactors. One such configuration is the field-reversed theta pinch, in which the current required to reverse the magnetic field on axis and create a closed magnetic field-line configuration is carried by the plasma. Unlike another type of compact toroid, the spheromak, there is no toroidal magnetic field in the field-reversed theta pinch. In creating a field-reversed theta pinch, a cylindrical chamber is filled with plasma in an initial, or bias, axial magnetic field; then an external current is applied which produces an axial magnetic field in the opposite direction of the initial bias field. As a result, an azimuthal current is induced in the plasma, the plasma is compressed by the resultant $\vec{J} \times \vec{B}$ force, and much of the initial bias flux is trapped. The resulting configuration is a long cylindrical plasma with an azimuthal current producing a region of closed field lines.

Immediately after compression in the field-reversed theta pinch, the equilibrium current is carried primarily by the electrons and the ions are approximately in a non-rotating thermal (Maxwellian) distribution. However, for reasons that are not yet well understood, at a later time the ions begin to rotate. If this ion rotation, or spin-up, is sufficiently large, rotational instabilities may result. These instabilities normally take the form of an $m=2$ mode, where m is the azimuthal mode number, corresponding to an elliptical deformation of the plasma cross-section. Such instabilities have been observed in experiments in Garching¹, Osaka², and Los Alamos³ shortly before the plasma is lost.

Magnetohydrodynamic theory predicts that rigidly rotating theta pinch equilibria will be unstable for any finite amount of ion rotation⁴. Results from fluid theory

which include finite Larmor radius corrections, have shown that these equilibria will be stable to rotational modes if the electrons and ions carry current in the same direction⁵. The results of Freidberg and Pearlstein⁵, using finite Larmor radius fluid theory, also demonstrate that growth rates for these instabilities are substantially less than those obtained from ideal magnetohydrodynamics.

A weakness of finite Larmor radius fluid theory is that it does not include the destabilizing effects of resonant ions, ions moving with the wave. Resonant ion effects can be significant when the Alfvén speed is comparable to or less than the ion thermal velocity. Seyler and Freidberg⁶ have shown that, for one-dimensional screw pinch equilibria, resonant particle effects can produce instability in regions of parameter space for which finite Larmor radius fluid theory predicts stability. The result of these calculations⁶ was to demonstrate that a regime which is magnetohydrodynamically unstable will still be unstable when kinetic effects are included, although the growth rate may be substantially reduced; i.e., there is no absolute finite Larmor radius stabilization. Similar results have been obtained by Finn and Sudan⁷ for the stability of thin ion rings immersed in a background plasma.

For non-reversed theta pinch equilibria the effects of resonant ions are expected to be small⁸. However, for strongly reversed cases, resonant ions may play an important role because near the field null the ion Larmor radius becomes very large. The lowest thresholds in terms of ion rotation and the largest growth rates for $m=2$ rotational instabilities occur when the axial wave number, k_z , is equal to zero. If k_z is sufficiently large, unstable rotational modes may be stabilized because of the influence of magnetic field line bending. Seyler⁹ found, using a Vlasov-fluid model, that the contribution of resonant ions increased the value of k_z required for stabilization rela-

tive to the results of finite Larmor radius fluid theory. Similarly, for some cases corresponding to theta pinches with significant field-reversal, Seyler⁹ found instabilities to occur at a lower value of ion rotation than finite Larmor radius theory predicted.

In this paper we study rotational instabilities with a two-dimensional, fully nonlinear, quasineutral hybrid simulation code. Axial variation is neglected (i.e., $k_z=0$). Ions are treated as particles so that both the stabilizing contribution of finite Larmor radius and the destabilizing contribution of resonant ions are included. Section II briefly describes the numerical model. The results of our simulations are presented in Section III.

II. SIMULATION MODEL

The simulation code that we have used to study rotational instabilities in the field-reversed theta pinch is a two-dimensional, fully nonlinear, quasineutral hybrid code. Our simulation code has been used previously to study kink instabilities in long ion layers¹⁰ and rotational instabilities in non-reversed theta pinch equilibria¹¹. Similar models have been used in one-dimensional problems by Byers et al.¹² and in two-dimensional (r,z) studies of theta pinch implosions by Hewett¹³. Ions are treated as particles to provide a fully kinetic description of their behavior. Since the time scales of rotational instabilities are much longer than the ion cyclotron period, it is unnecessary to follow the details of the electron dynamics. Hence, the electrons are considered to be an inertialess fluid. In addition, electromagnetic radiation effects are not important on these time scales, allowing us to use the Darwin version of Ampere's law (i.e., the transverse displacement current is neglected).

The Darwin version of Ampere's law is combined with the inertialess version of

the electron momentum equation and the assumption of quasineutrality to determine the electric field. In these simulations we assume that the electrons are cold. The expression for the electric field (as derived in Ref. 11) is

$$\vec{E} = \frac{1}{4\pi n_i e} (\nabla \times \vec{B}) \times \vec{B} - \frac{1}{n_i e c} \vec{J}_i \times \vec{B}. \quad (1)$$

In Eq. 1 the ion density, n_i , and the ion current density, \vec{J}_i , are determined from the ion particles by linear weighting (particle-in-cell) from the grid. The magnetic field is advanced in time by Faraday's law and the ions are moved by the equations of motion.

The equations are solved in the $r-\theta$ plane. However, for numerical reasons, Cartesian coordinates are used in the simulation. No axial variation is allowed (i.e., $\partial/\partial z=0$) and B_x , B_y , E_z , J_z , and v_z are all set equal to zero. Square conducting wall boundaries are used. The vacuum electric field is determined by solving $\nabla^2 \vec{E}=0$ in the vacuum regions, while the vacuum magnetic field is determined by assuming vacuum flux conservation. A more detailed description of this code may be found in Ref. 11.

Our simulations begin with the loading of a Vlasov equilibrium (i.e. $\partial f_0/\partial t=0$) theta pinch distribution, corresponding to an exponential rigid rotor¹⁴,

$$f(r, v_r, v_\theta) = \frac{n_0}{\pi v_i^2} \text{sech}^2 \left(\frac{r^2 - r_1^2}{r_0^2} \right) \left[-\frac{v_r^2 + (v_\theta - r\Omega_i)^2}{2v_i^2} \right]. \quad (2)$$

In this distribution, v_i is the ion thermal velocity, Ω_i is the mean ion rotational frequency, r_1 is the major radius, and r_0 is a measure of the minor radius of the plasma. This distribution gives the current density profile

$$J_\theta(r) = -en_0\Omega_i \text{sech}^2 \left(\frac{r^2 - r_1^2}{r_0^2} \right) \quad (3)$$

and the magnetic field profile

$$B_z(r) = \frac{cm_i\Omega_i^2}{e\Omega_*} + \frac{cm_iv_i^2}{e\Omega_*r_0^2} \tanh\left(\frac{r^2-r_1^2}{r_0^2}\right). \quad (4)$$

m_i is the ion mass, Ω_e is the mean electron frequency, and Ω_* is the frequency of the relative drift between the ions and electrons, $\Omega_* \equiv \Omega_e - \Omega_i$. We initialize our simulations by specifying r_1 , r_0 , Ω_i , and Ω_e . The ion thermal velocity is then given by

$$v_i = \frac{r_0}{2} \left(\omega_{ci} \Omega_* - \Omega_i^2 \right)^{\frac{1}{2}}. \quad (5)$$

For simulations with rotating ions we assume the ions are in an initially rotating equilibrium as might exist in the later stages of an experiment like FRX-B at Los Alamos³. Unstable modes are naturally excited in our simulations by the thermal noise in the initial equilibrium. We do not attempt to model the mechanism which causes the onset of rotation.

The assumption that the electrons are cold is justified, since in both the FRX-B experiment³ and in the PIACE experiment² in Osaka the dominant contribution to the plasma pressure comes from the ions. This is not always the case, as in the experiment at Kurchatov¹⁵ where the electron and ion temperatures are comparable.

The simulations discussed in the following section represent the ions with 50,000 particles and spatial finite differencing is performed on a 100 by 100 grid.

III. RESULTS

A. Linear Growth Rates

Our simulation code has been applied previously to non-reversed rotating theta pinch equilibria¹¹. These equilibria are in the parameter range studied by Freidberg

and Pearlstein⁵ and by Seyler⁹. The effects of resonant particles on rotational instabilities should be relatively small for the non-reversed case. This accounts for the similarity between the results of Seyler's Vlasov-fluid model and the finite Larmor radius fluid model of Freidberg and Pearlstein. Our simulations for the non-reversed case¹¹ showed comparable growth rates for the $m=2$ mode to those predicted by these previous theories.

The goal of this work is to examine by numerical simulation the behavior of rotational modes for equilibria in which resonant ion effects may be significant, i.e., equilibria with substantial field-reversal. As in previous papers^{5,9}, we define a parameter $\alpha \equiv -\Omega_i/\Omega_e$ and a parameter β_0 , the "beta-on-axis", as $\beta_0 = 8\pi n(0) T_i / B_0^2$. T_i is the ion temperature, $T_i = (1/2) m_i v_i^2$, and B_0 is the external magnetic field. A theta pinch equilibrium with the ions in a non-rotating Maxwellian distribution (i.e., $\alpha=0.0$) with $\Omega_e = 0.05\omega_{ci}$ (ω_{ci} is the ion cyclotron frequency in the external magnetic field) and $\beta_0 = 0.65$ corresponds to field-reversal of 60%, i.e. $|B_z(0)/B_0| = 0.6$. This value of β_0 is comparable to the values measured in typical FRX-B experiments. The experimental density and temperature measurements used to determine β_0 are normally taken prior to the onset of ion rotation and the growth of the resulting $m=2$ instability. If $|B_z(0)/B_0|$ remain constant during the spin-up of the ions, i.e., as α increases, β_0 must decrease. This decrease in β_0 to maintain equilibrium is required to compensate for the centrifugal force due to the ion rotation. In the PIACE experiment at Osaka², a magnetic probe is placed on axis to measure the value of $B_z(0)$. In PIACE it is found that the magnetic field on axis remains approximately constant throughout the lifetime of the experiment. Therefore, in our simulations we vary α while keeping $|B_z(0)/B_0|$ fixed, rather than fixing β_0 , in order to find the growth rates for different

amounts of ion rotation. The effect of ion rotation on β_0 is substantial. When the above parameters are substituted into the rigid rotor distributions of Section II, we find that when $\alpha=1.0$, to achieve 60% field-reversal, $\beta_0=0.49$ rather than $\beta=0.65$ when $\alpha=0.0$. Figure 1 summarizes the growth rates for the $m=2$ mode as determined from simulations for different values of α with 60% field-reversal and $\Omega_* = 0.05\omega_{ci}$. Figure 2 shows the real frequencies, ω_r , obtained from simulations using these parameters. Our results in Fig. 1 are markedly different than those of finite Larmor radius fluid theory, which predict stability for $\alpha < 1.0$.

The lowest value of α in Fig. 1 for which the $m=2$ instability has been clearly observed in our simulations is $\alpha=0.4$. This is identical to the value of rotation measured from carbon impurities in FRX-B at the onset of the $m=2$ instability³. However, for $\alpha=0.4$ our simulations give a growth rate, $\gamma=0.011\omega_{ci}$, which appears to be slightly low in order to account for the gross distortion of the plasma observed to occur in experiments in less than $4 \mu s$ after the instability first appears (for deuterium, $B_0=8 kG$, and $\gamma=.011\omega_{ci} \exp(\gamma t)=\exp(0.42 t(\mu s))$). Recently there has been some uncertainty as to whether the carbon measurements are an accurate indicator of the rotation velocity of the deuterium ions¹⁶. Therefore, the experimental value of $\alpha=0.4$ for instability should be considered only as an estimate. When the carbon measurements are taken, α is increasing. One possibility is that $\alpha \approx 0.4$ when the elliptical deformation of the plasma is first observed and then, as the instability grows, α continues to increase to larger values. From simulations we find that $\gamma=0.29\omega_{ci}$ for $\alpha=0.8$. If α was to increase so that it approached or exceeded 0.8, the growth rate for the $m=2$ mode, taken from our simulations, might account for the rapid instability growth seen in FRX-B (for deuterium, $B_0=8 kG$, and $\gamma=0.029\omega_{ci}$

$$\exp(\gamma t) = \exp(1.10 t(\mu s)).$$

The value of β_0 , which serves as a measure of the peakedness of the density profile, has been found to be a critical factor in rotational stability. Figure 3 shows growth rates for the $m=2$ mode as a function of β_0 with $\alpha=1.0$ and $\Omega_e=0.05\omega_{ci}$. One can see that growth rates increase with decreasing β_0 . This is an indication of a resonant particle effect because distributions which are sharply peaked off axis have a larger number of ions near the field null than do distributions with flatter profiles.

The results of the Vlasov-fluid model of Seyler⁹, which includes the effects of resonant ions, have shown that an unstable mode exists for α as low as 1.3, in a parameter regime where finite Larmor radius fluid theory predicts $m=2$ stability for $\alpha < 1.6$. This lower unstable value of α was presumed to be due to the destabilizing contribution of resonant ions. This reference did not predict instability for $\alpha < 1.3$, such as found here. A possible reason for this omission was that the eigenvalues considered were for instabilities where fluid effects, rather than resonant ion effects, play the dominant role¹⁷; the eigenfunctions for the modes (described in Ref. 9) increase monotonically with radius in the plasma so that they have their maximum perturbation at the plasma edge, as is characteristic of Rayleigh-Taylor-like instabilities. Although our simulation diagnostics do not provide a precise description of the eigenfunction, our contour plots show that the maximum perturbation for the unstable modes observed in our simulations lies near the field null, rather than near the plasma edge. An eigenfunction peaked near the field null is an indication that resonant ions are important, since their effects are strongest there.

Recently, Seyler has applied the Vlasov-fluid model to parameters like those used in our simulations¹⁷; he has duplicated our result that unstable $m=2$ modes do exist

for $\alpha < 1$. Using slightly different parameters than we have simulated, Seyler has found the existence of unstable $m=2$ modes at $\alpha=0.6$ and $\alpha=0.4$. For one set of parameters that are identical to those used in one of our simulation runs, the Vlasov-fluid model gives $\omega_r=0.051\omega_{ci}$ and $\gamma=0.022\omega_{ci}$; from our simulation we estimate $\omega_r=0.070\omega_{ci}$ and $\gamma=0.039\omega_{ci}$. The values of the growth rate and real frequency obtained for these parameters from the Vlasov-fluid model are somewhat lower than those obtained from our simulation. However, as seen in our simulations, the eigenfunctions for this mode at $\alpha=1.0$ and for other modes with $\alpha < 1.0$ found with the Vlasov-fluid model¹⁷ are peaked near the field null, unlike earlier results^{5,9} described above.

One possible source for the discrepancy in growth rate between the new results of Seyler and our results is the existence of another unstable mode which has a low saturation level. Seyler has found¹⁷ that another unstable mode exists having a much higher growth rate with an eigenfunction peaked near the plasma edge. While we have not observed such a mode as yet in our simulations, if this mode was present it might be difficult with our diagnostics to isolate its behavior prior to saturation from the mode which causes the gross distortion of the plasma over long times. This could alter our growth rate measurements and explain the discrepancy. Another possible source of the discrepancy could be slight differences between the initialization of the rigid rotor equilibrium in our simulations and the rigid rotor equilibrium used by Seyler^{9,17}.

B. Long-Time Behavior

In this section we present the results of a simulation that has been allowed to run

well into the nonlinear stage of an $m=2$ rotational instability. The parameters for this simulation are $\beta_0=0.49$, $\Omega_0=0.05\omega_{ci}$, and $\alpha=1.0$. The distance of the conducting wall from the center of the system is $r_w=6r_1$. These parameters give $|B_z(0)/B_0|=0.6$ and $S=8.3$. S is defined to be $S=r_1/\rho_i$, the ratio of the plasma major radius to the ion Larmor radius in the external field ($\rho_i=v_i/\omega_{ci}$). The value of S in this simulation is comparable to the value in some FRX-B experiments.

Figures 4 and 5 show the initial density and magnetic field profiles for this simulation. Figures 6a-6f show the particle positions in the $r-\theta$ plane for the initial distribution and the subsequent distributions at successive time intervals of $60\omega_{ci}^{-1}$. Typically in FRX-B, $\omega_{ci}\approx 3.8\times 10^7 s^{-1}$, so that these time intervals would be equal to $1.6\ \mu s$ in real time. The growth of the $m=2$ instability is clear and by $t=300\omega_{ci}^{-1}$ (Fig. 6f) the plasma cross-section has become grossly distorted. As the instability becomes highly nonlinear, the growth rate decreases so that by the end of this run, $t=320\omega_{ci}^{-1}$, the plasma has not been driven to the walls. This point in time would correspond to approximately $8\ \mu s$ in FRX-B, which is roughly equal to the experimental lifetime of the plasma after the $m=2$ instability is first observed. We define a parameter $\delta r(\theta, t)$ as the difference between the average ion radius at a given angle and the initial average ion radius, $\delta r(\theta, t)=\langle r(\theta, t) \rangle - \langle r(\theta, 0) \rangle$. $\delta r(\theta)$ is stored at time intervals and then decomposed into its azimuthal Fourier components. Figure 7 shows $(\delta r(t))^2$ for the $m=2$ mode from $t=0$ to $t=200\omega_{ci}^{-1}$. The decrease in the growth rate with time is evident in Fig. 7. This type of behavior, the reduction of the growth rate, slowing the total disruption of the plasma, has been observed in experiments in both PIACE² and FRX-B¹⁶. In these experiments the plasma cross-section has often been observed to evolve into a rotating elliptical shape which continues to deform, but not

exponentially, and never actually drives the plasma to the walls during the lifetime of the plasma. These observations are consistent with our simulations.

Another observation concerning the nonlinear behavior of the $m=2$ instability in our simulations is the reduction in the real frequency, ω_r , of the mode as it grows to large amplitude. In the simulation described above, we have measured the real frequency when we first observe the instability as $\omega_r=1.38\Omega_*$. However, this frequency steadily decreases as the mode grows until it reaches $\omega_r=0.3\Omega_*$ near the end of the simulation. The real frequency is plotted as a function of time in Fig. 8. Although the parameters in PIACE generally correspond to a higher value of Ω_* than used in this simulation run, the frequency decrease observed in our simulation is qualitatively very close to that reported in Ref. 2. The same type of decrease in ω_r has also been observed in FRX-B¹⁶.

C. Reduced Compression

The lifetimes of field-reversed theta pinch experiments in the past have been found to increase when the magnetic compression factor, K , is reduced; K is defined by $K\equiv|B_f/B_i|$, where B_i is the initial bias field and B_f is the final external magnetic field ($B_f=B_0$). When K is reduced, the initial bias field is increased relative to the final external field, hence, the amount of bias magnetic flux trapped, and consequently the amount of field-reversal on axis, is increased. As the degree of field-reversal is increased (i.e., K decreased) the equilibrium plasma pressure at the separatrix must decrease. Although the precise reason for the improved lifetime with small values of K is uncertain, one possible explanation is that the reduced density near the separatrix decreases the loss of ions to open field lines, which may reduce the spin-up of the

ions.

We have made several simulation runs in an attempt to see the effect of reducing the magnetic compression on rotational instabilities. The results in Fig. 3 indicate that when β_0 is reduced, corresponding to decreased compression, then growth rates increase. When we examine values of β_0 below those of Fig. 3, $\beta_0 \leq 0.4$, we find that instabilities have larger growth rates at smaller values of α than were found when $\beta_0 \approx 0.6$.

For a plasma with $|B_z(0)/B_0|=0.75$, corresponding to $\beta_0=0.4$ when $\alpha=0.0$, we have made runs for $\alpha=0.5$ and $\alpha=1.0$. For these parameters $S \approx 10$. At $\alpha=0.5$ ($\beta_0=0.36$), as in our simulations with $|B_z(0)/B_0|=0.60$, we find an $m=2$ instability. However, the measured growth rate for this simulation, $\gamma=0.035\omega_{ci}$, is considerably larger than that for the simulation with 60% field-reversal, where $\gamma=0.011\omega_{ci}$. For $\alpha=1.0$ ($\beta_0=0.23$) the $m=2$ mode is unstable, but now an unstable $m=3$ mode is also present and dominates the plasma behavior. The $m=3$ mode is evident in the particle position plot at $t=110\omega_{ci}^{-1}$ shown in Fig. 9. The measured growth rate for the $m=3$ mode is $\gamma=0.036\omega_{ci}$ and the measured $m=2$ growth rate is $\gamma=0.024\omega_{ci}$. For simulations with still stronger field-reversal we have also observed $m=4$ and $m=5$ instabilities. Therefore, for the same value of ion rotation we would expect to see faster growing instabilities with larger azimuthal mode numbers as the compression factor is reduced.

Recently, experiments have been performed on FRX-B with reduced compression²⁰ so that $\beta_0 \approx 0.4$. In these experiments it was observed that:

1. Unstable modes with $m > 2$ were considerably more common than in the earlier shots with higher compression¹⁸.
2. The stable period was typically 15% longer in time than in the higher compression shots²⁰.

The first result is consistent with our simulations which did not exhibit instabilities with $m > 2$ when $|B_z(0)/B_0|=0.6$, but did with $|B_z(0)/B_0|=0.75$. The second result could be due to the fact that the reduction in ion losses to open field lines in the reduced compression case has decreased the spin-up of the ions. The decreased spin-up would increase the length of time for the plasma to reach a given value of α with a large growth rate. Therefore, even though growth rates in this case are larger for a fixed value of α , the decrease in spin-up may prevent the appearance of instabilities at early times in experiments with low magnetic compression.

The FRX-C experiment, which is an upgrade from FRX-B, is being designed to operate in a range of magnetic compression similar to the latest low compression experiments on FRX-B. FRX-C is larger, having a wall radius of 20 cm rather than the 10 cm wall radius of FRX-B. The intent in FRX-C is to increase the parameter $S=r_1/\rho_i$ to further decrease transport losses. FRX-C has been designed to operate in a parameter range with $\beta_0 \approx 0.3-0.4$ and $S \approx 20-40$. One effect of this increase in S is to reduce the drift frequency, Ω_{\perp} . Therefore, for a given $\alpha > 0$, Ω_{\perp} will be less than in the high compression case so that the centrifugal forces of the rotating ions will be negligible. Hence, in this case, the density profile will not become substantially more peaked (i.e., β_0 will not be significantly reduced) as spin-up occurs.

We have simulated a rotating theta pinch with parameters like those of FRX-C. For this simulation $|B_z(0)/B_0|=0.82$ and $\Omega_{\perp}=0.005\omega_{ci}$. We assume ion rotation such

that $\alpha=1.0$. These parameters give a rigid rotor equilibrium with $\beta_0=0.3$ and $S=31$. From the simulation we estimate the growth rate for the $m=2$ mode to be $\gamma=0.0026\omega_{ci}$ and for the $m=3$ mode $\gamma=0.0072\omega_{ci}$, which are much less than the growth rates estimated from our simulations using low compression FRX-B parameters.

It is hoped that FRX-C will have a longer lifetime because the increase in S , combined with low compression, will reduce the loss of ions to open field lines and consequently reduce ion spin-up, so that α will remain near zero. Our simulations provide a new result, favorable for FRX-C, that instability growth rates for a given value of α in FRX-C should be much less than in FRX-B.

IV. Conclusions

We have used a quasineutral hybrid simulation code to study instabilities in rigidly rotating field-reversed theta pinch equilibria. We have found the $m=2$ instability to occur at levels of ion rotation that were previously thought to be stable from finite Larmor radius fluid theory. Even though there is uncertainty concerning the experimental measurement of ion rotation, measurements from carbon impurities indicate a value of unstable ion rotation much closer to our simulations than to the results of finite Larmor radius fluid theory. Our result, that the $m=2$ instability should occur for $\alpha < 1.0$, has been confirmed by the Vlasov-fluid model of Seyler¹⁷.

Our simulation model and the Vlasov-fluid model both include the effects of resonant ions, absent in finite Larmor radius fluid theory. Because we find that for modes with $\alpha < 1.0$ that growth rates decrease with decreasing Larmor radius, and that their eigenfunctions are peaked near the field null rather than near the plasma edge, it

appears that resonant ions may be the dominant driving force for these instabilities. Our results (Fig. 1) are an indication that, as in other configurations^{6,7}, absolute finite Larmor radius stabilization may not occur for rotational instabilities in the field-reversed theta pinch.

We have found that both the growth rate and the real frequency of the $m=2$ mode decrease at large amplitude. This behavior is similar to that observed in experiments at Osaka and Los Alamos.

For cases with decreased compression we find that growth rates for low values of α are larger than in high compression cases. We also find that in low compression cases, modes with $m > 2$ can be unstable for $\alpha=1.0$. However, in a result favorable for the FRX-C experiment, we find that increasing $S=r_1/\rho_i$ can produce a large reduction in the growth rates for the unstable modes.

ACKNOWLEDGMENTS

The author is indebted to Prof. C.K. Birdsall for his discussions, advice, and encouragement during the course of this work. The author acknowledges Dr. C.E. Seyler who provided invaluable assistance in the comparison of our results with those of the Vlasov-fluid model. Many valuable discussions were also held with Drs. D.W. Hewett, M. Tuszewski, and R.K. Linford.

This work was supported by ONR Contract No. N00014-17-C0578. Computations were performed at the National Magnetic Fusion Energy Computer Center at Livermore.

REFERENCES

1. A. Eberhagen and W. Grossman, "Theta Pinch Experiments with Trapped Antiparallel Magnetic Fields", *Z. Physik* **248**, pp. 130-149 (1971).
2. S. Ohi, S. Okada, M. Tanjo, Y. Ito, T. Ishimura, and H. Ito, "A keV Compact Toroidal Plasma", Proceedings of the Third Symposium on Physics and Technology of Compact Toroids in the Magnetic Fusion Energy Program, pp. 192-195 (Los Alamos, 1980).
3. R.K. Linford, W.T. Armstrong, D.A. Platts, and E.G. Sherwood, "Field Reversal Experiments (FRX)", Proceedings of the Seventh IAEA Conference on Plasma Physics and Controlled Thermonuclear Research", pp. 447-456 (Innsbruck, 1978).
4. J.B. Taylor, "Rotation and Instability of Plasma in Fast B_z Compression Experiments", *J. Nucl. Energy Pt. C* **4**, pp. 401-407 (1962).
5. J.P. Freidberg and L.D. Pearlstein, "Rotational Instabilities in a Theta Pinch", *Phys. Fluids* **21**, pp. 1207-1217 (1978).
6. C.E. Seyler and J.P. Freidberg, "Resonant Particle Effects on Finite Larmor Radius Stabilization", *Phys. Fluids* **23**, pp. 331-336 (1980).
7. J.M. Finn and R.N. Sudan, "Betatron Resonance Instabilities in Axisymmetric Field-Reversed Systems", *Phys. Fluids* **22**, pp. 1148-1153 (1979).
8. L.D. Pearlstein and J.P. Freidberg, "Finite Larmor Radius Equations in an Arbitrary Near-Theta Pinch Geometry", *Phys. Fluids* **21**, pp. 1218-1226 (1978).
9. C.E. Seyler, "Vlasov-Fluid Stability of a Rigidly Rotating Theta Pinch", *Phys. Fluids* **22**, pp. 2324-2330 (1979).

10. D.S. Harned, "Kink Instabilities in Long Ion Layers", in preparation for submittal to Phys. Fluids.
11. D.S. Harned, "Quasineutral Hybrid Simulation of Macroscopic Plasma Phenomena", in preparation for submittal to J. Comput. Phys.
12. J.A. Byers, B.I. Cohen, W.C. Condit, and J.D. Hanson, "Hybrid Simulation of Quasineutral Phenomena in Magnetized Plasma", J. Comput. Phys. 27, pp. 363-396 (1978).
13. D.W. Hewett, "A Global Method of Solving the Electron-Field Equations in a Zero-Inertia-Electron-Hybrid Plasma Simulation Code", J. Comput. Phys. 38, pp. 378-395 (1980).
14. R.C. Davidson, Theory of Nonneutral Plasmas, W.A. Benjamin Inc. (London, 1974).
15. A.G. Eskov, R.H. Kurtmullaev, A.P. Kreschuk, Ya.N. Laukhin, A.I. Malyatin, A.I. Markin, Yu.S. Martyushov, B.N. Mironov, M.M. Orlov, A.P. Proshletsov, V.N. Semenov, and Yu.B. Sosunov, "Principles of Plasma Heating and Confinement in a Compact Toroidal Configuration", Proceedings of the Seventh IAEA Conference on Plasma Physics and Controlled Thermonuclear Research, pp. 187-204 (Innsbruck, 1978).
16. R.K. Linford, private communication.
17. C.E. Seyler, private communication.
18. M. Tuszewski, private communication.
19. R.E. Siemon and R.R. Bartsch, "Scaling Laws for FRC Formation and Prediction of FRX-C Parameters", Proceedings of the Third Symposium on Physics and

- Technology of Compact Toroids in the Magnetic Fusion Energy Program, pp. 172-175.
20. W.T. Armstrong, J.C. Cochrane, J. Lipson, R.K. Linford, K.F. McKenna, A.G. Sgro, E.G. Sherwood, R.E. Siemon, and M. Tuszewski, "FRC Studies on FRX-B", Proceedings of the Third Symposium on Physics and Technology of Compact Toroids in the Magnetic Fusion Energy Program, pp. 180-183.

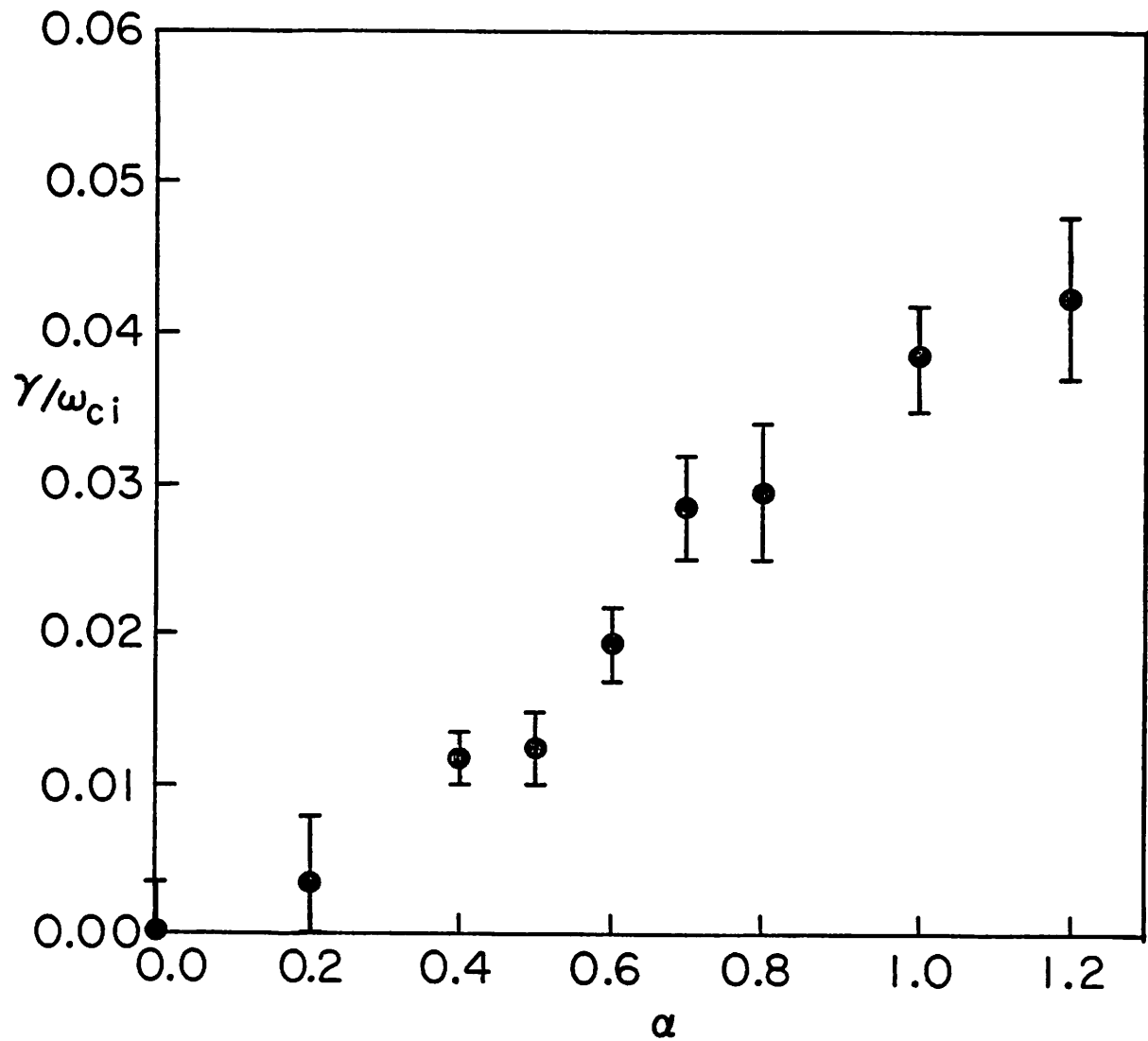


FIG. 1. Growth rates, γ , obtained from simulation for the $m=2$ mode as a function of α . $|B_z(0)/B_0|=0.6$ and $\Omega_e=0.05\omega_{ci}$. β_0 varies from 0.41 for $\alpha=1.2$ to 0.65 for $\alpha=0.0$.

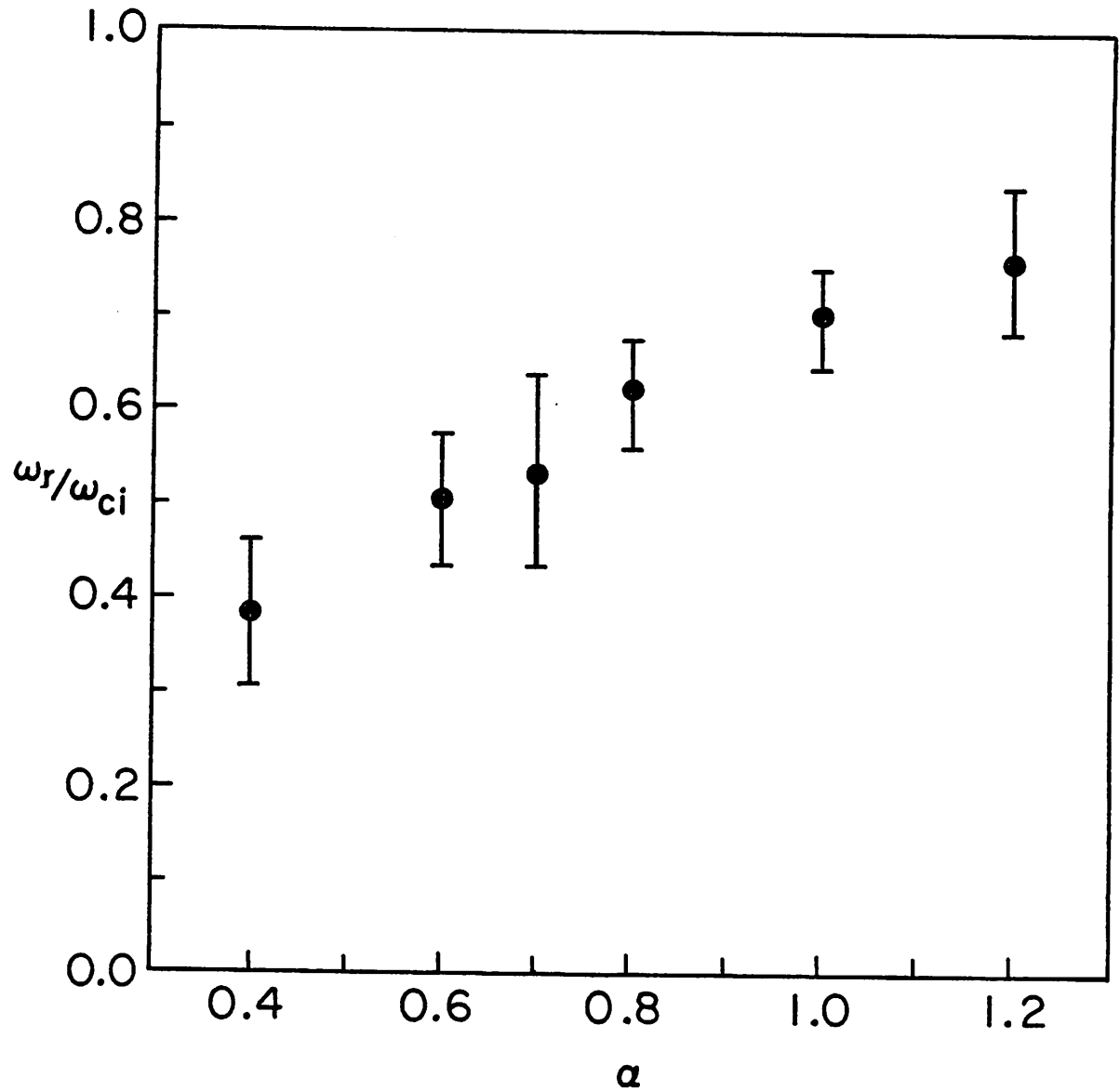


FIG. 2. Real frequencies, ω_r , obtained from simulation for the $m=2$ mode as a function of α . $|B_z(0)/B_0|=0.6$ and $\Omega_s=.05\omega_{ci}$.

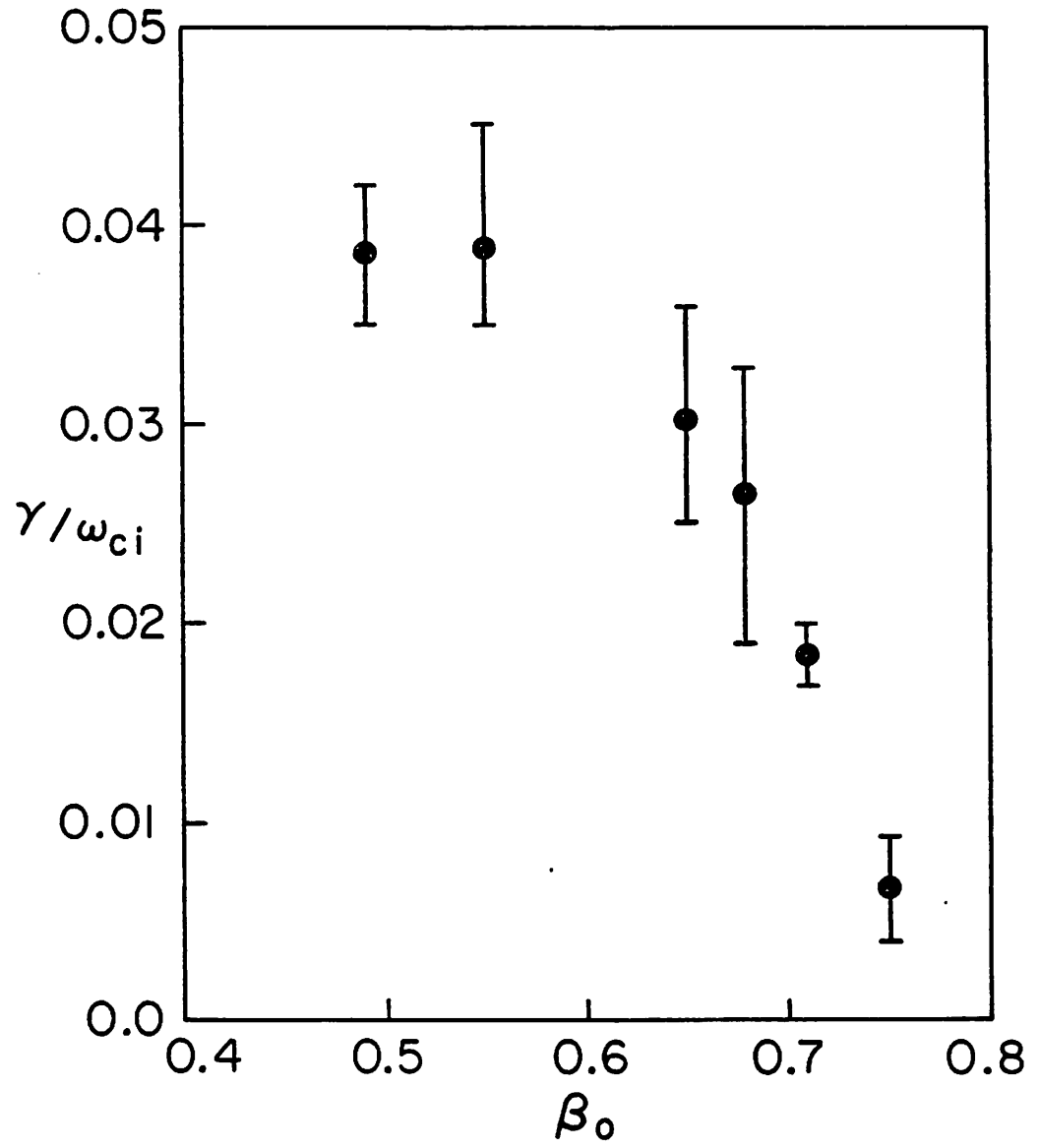


FIG. 3. Growth rates, γ , obtained from simulation for the $m=2$ mode as a function of β_0 . $\alpha=1.0$ and $\Omega_e=0.05\omega_{ci}$.

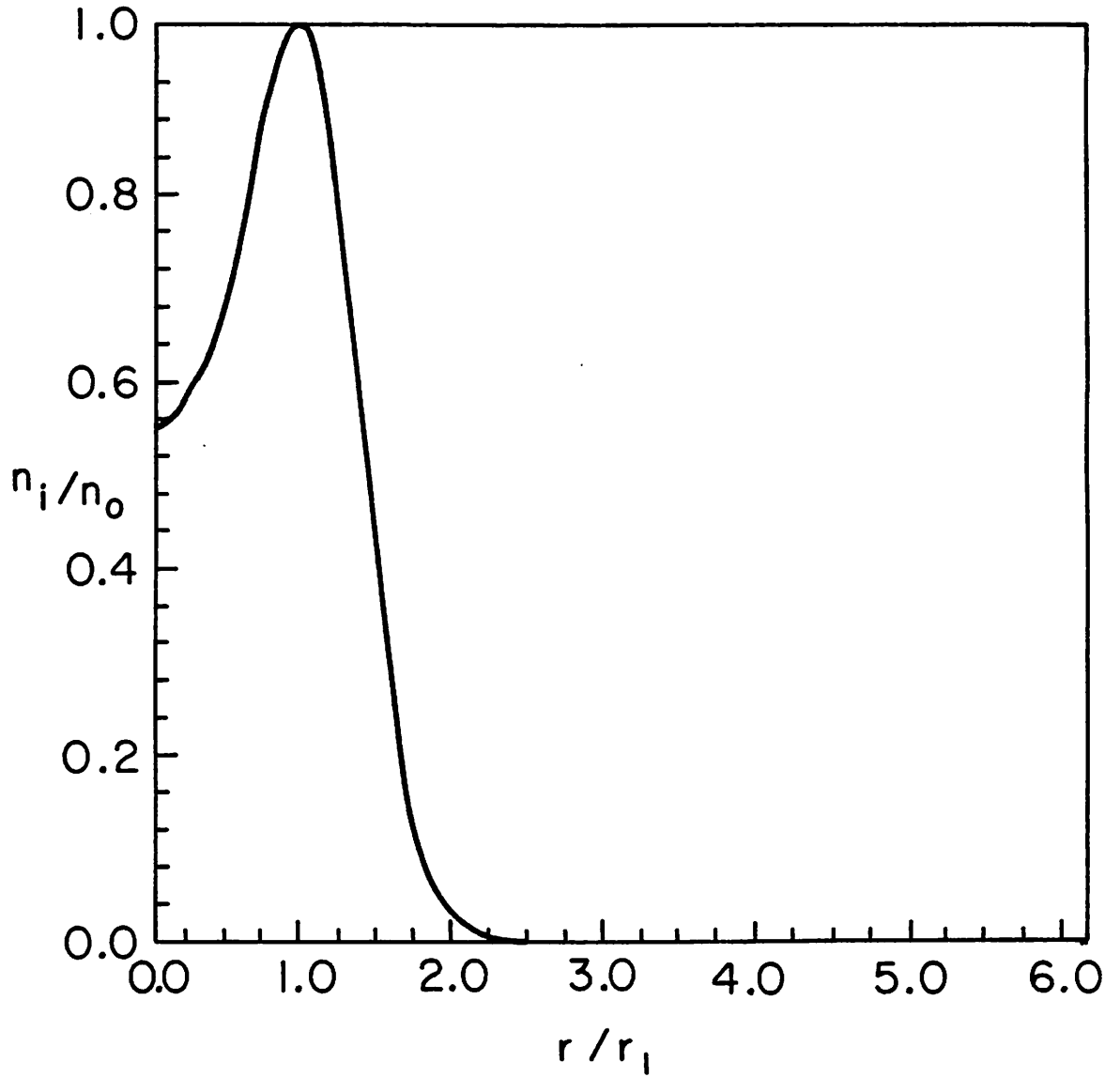


FIG. 4. Initial density profile, $n_i(r)$, for a simulation of a field-reversed theta pinch equilibrium, similar to some FRX-B experiments. $\Omega_e=0.05\omega_{ci}$, $\beta_0=0.49$, and $\alpha=1.0$.

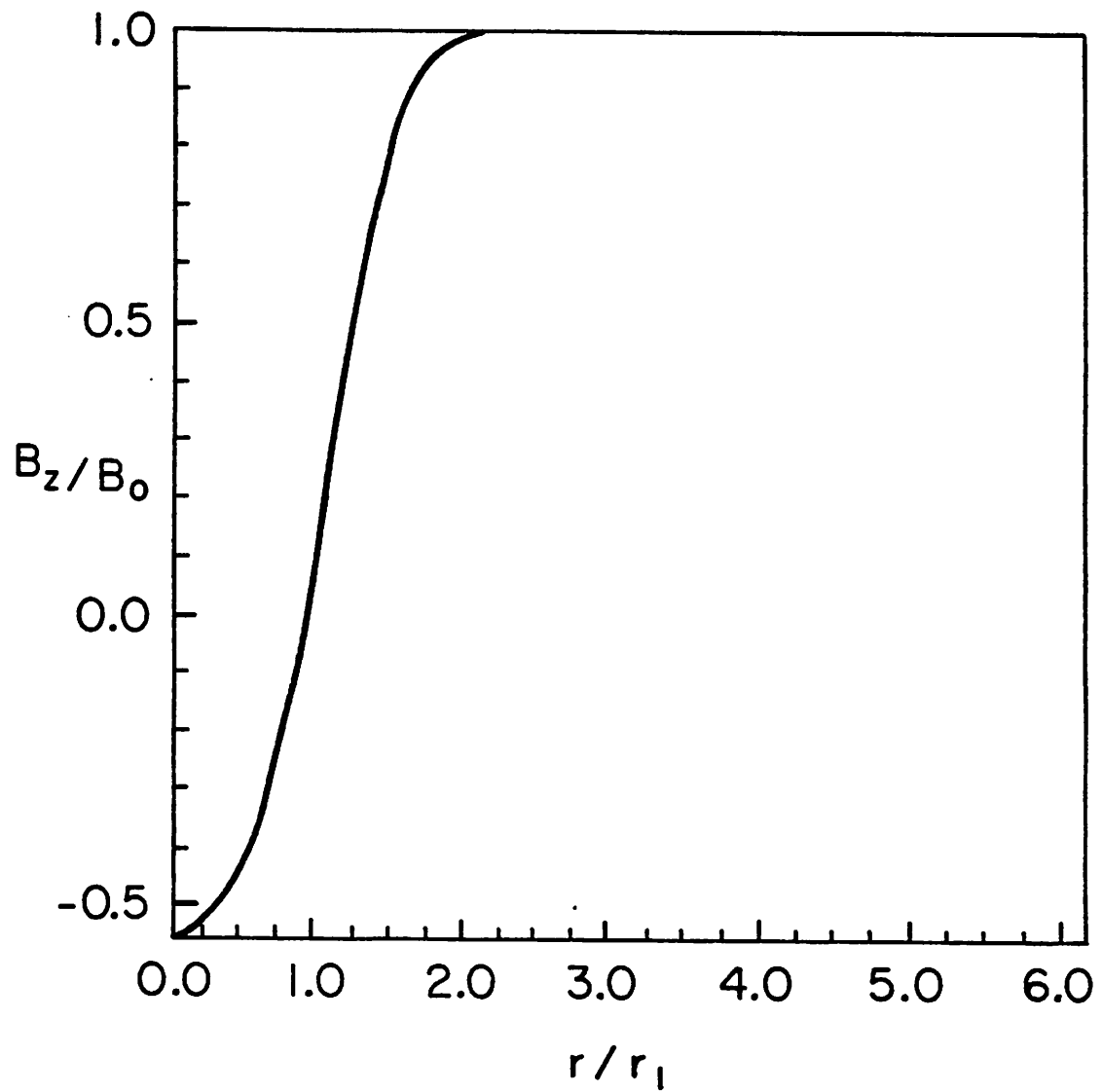


FIG. 5. Initial magnetic field profile, $B_z(r)$, for the equilibrium of Fig. 4.

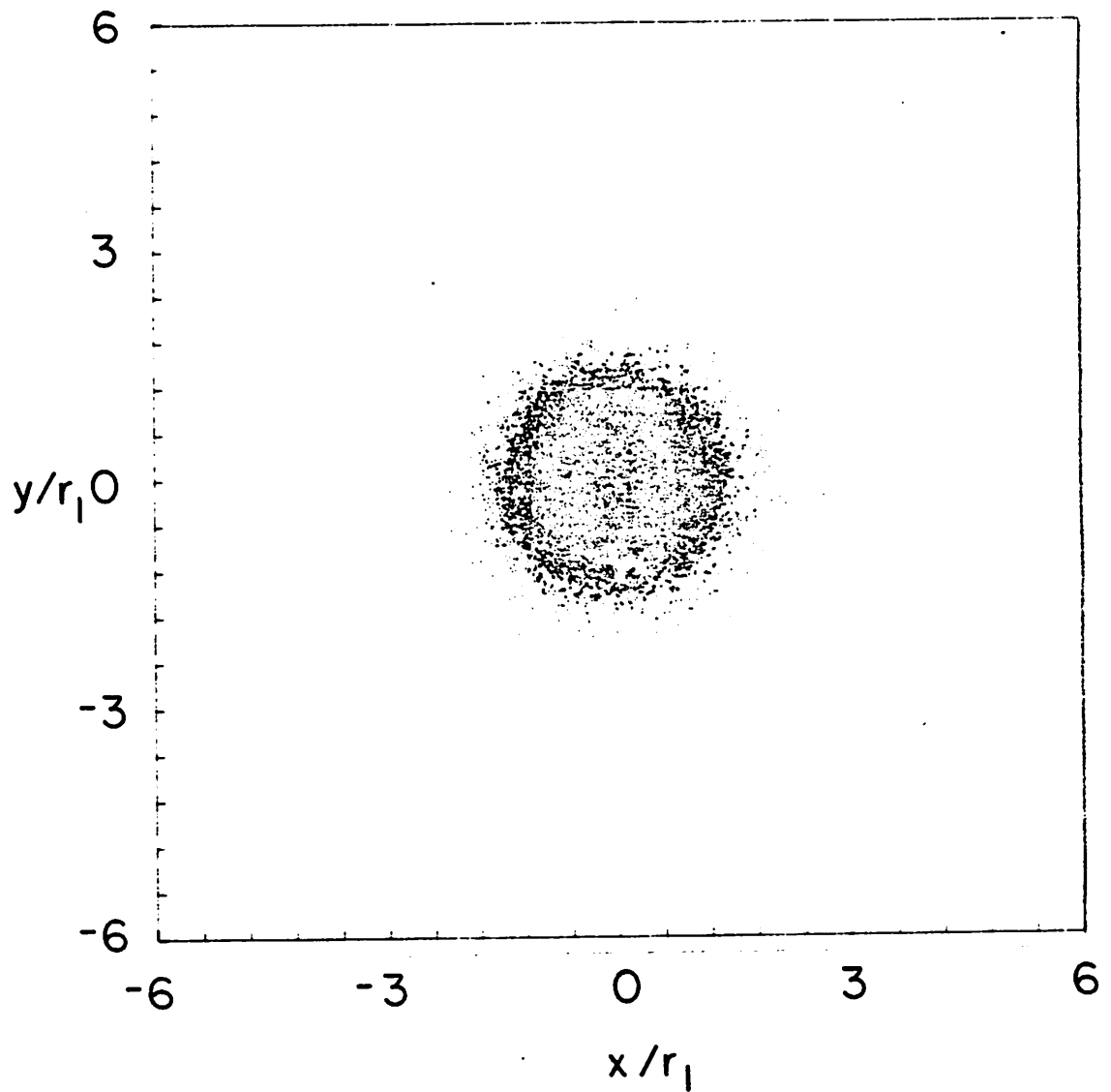


FIG. 6. Initial particle positions in the r - θ plane (6a) for the equilibrium of Fig. 4. Figs. 6b-6f show the particle positions at $t=60, 120, 180, 240,$ and $300 \omega_{ci}^{-1}$, respectively.

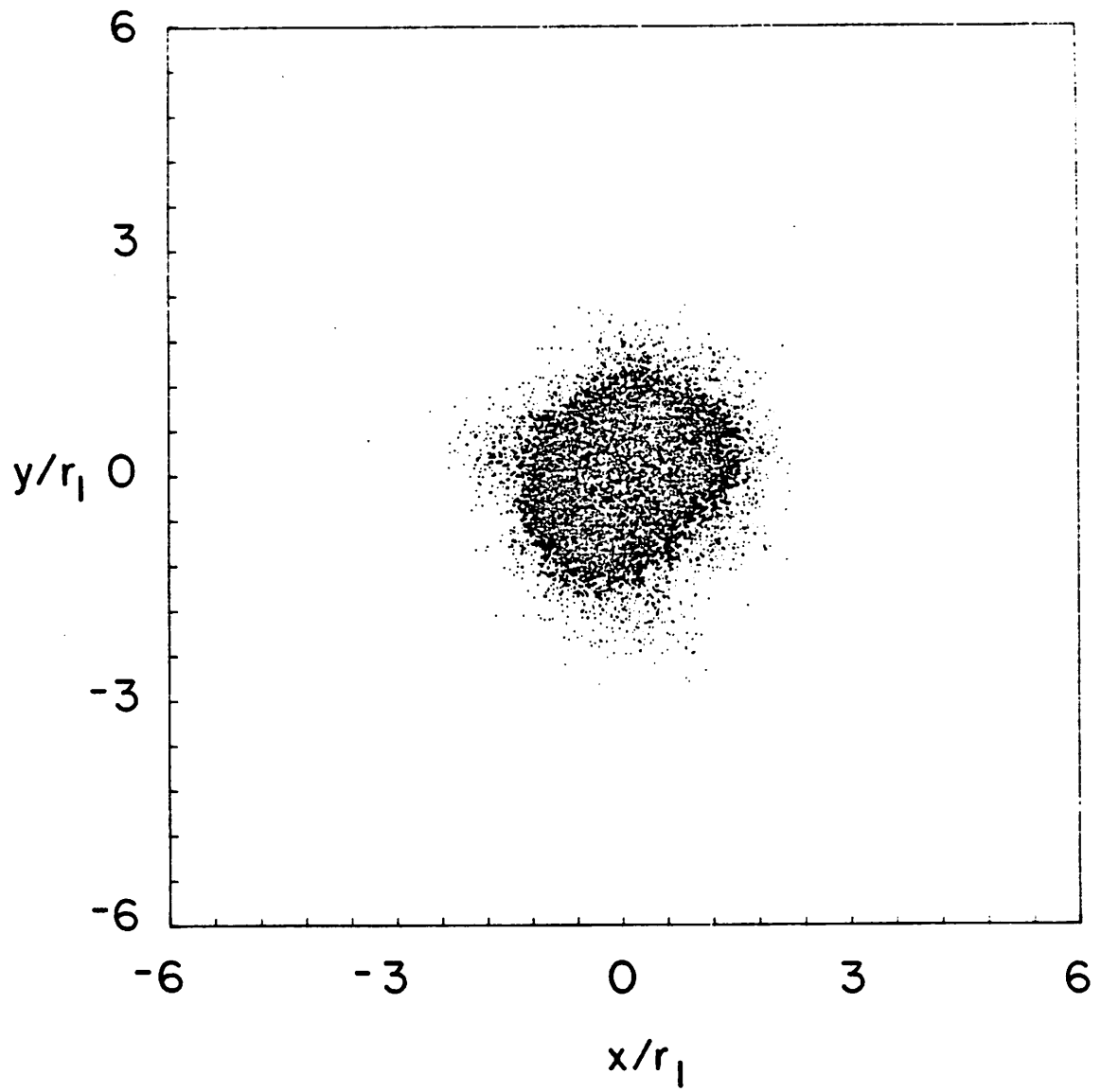


FIG. 6b.

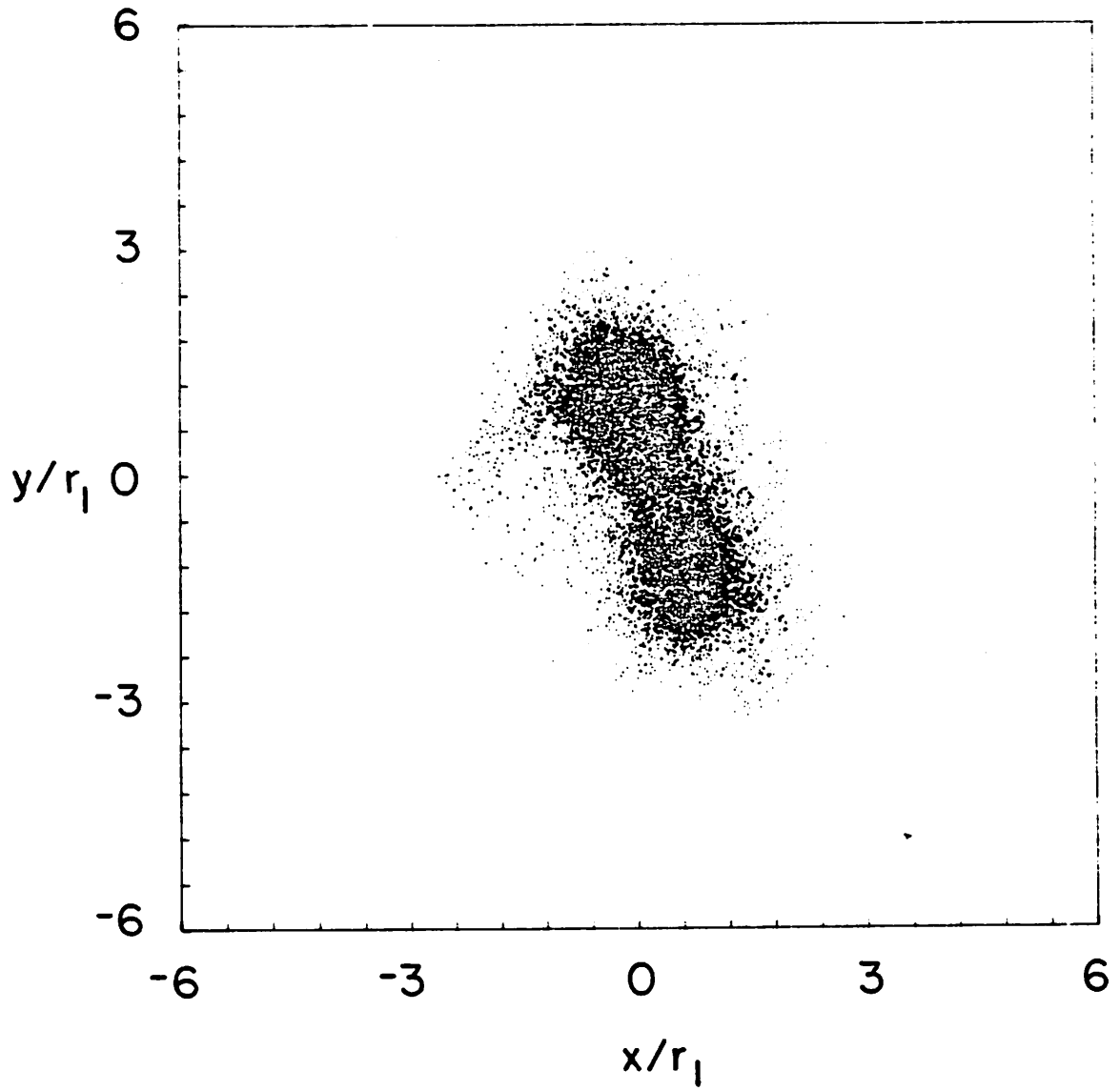


FIG. 6c.

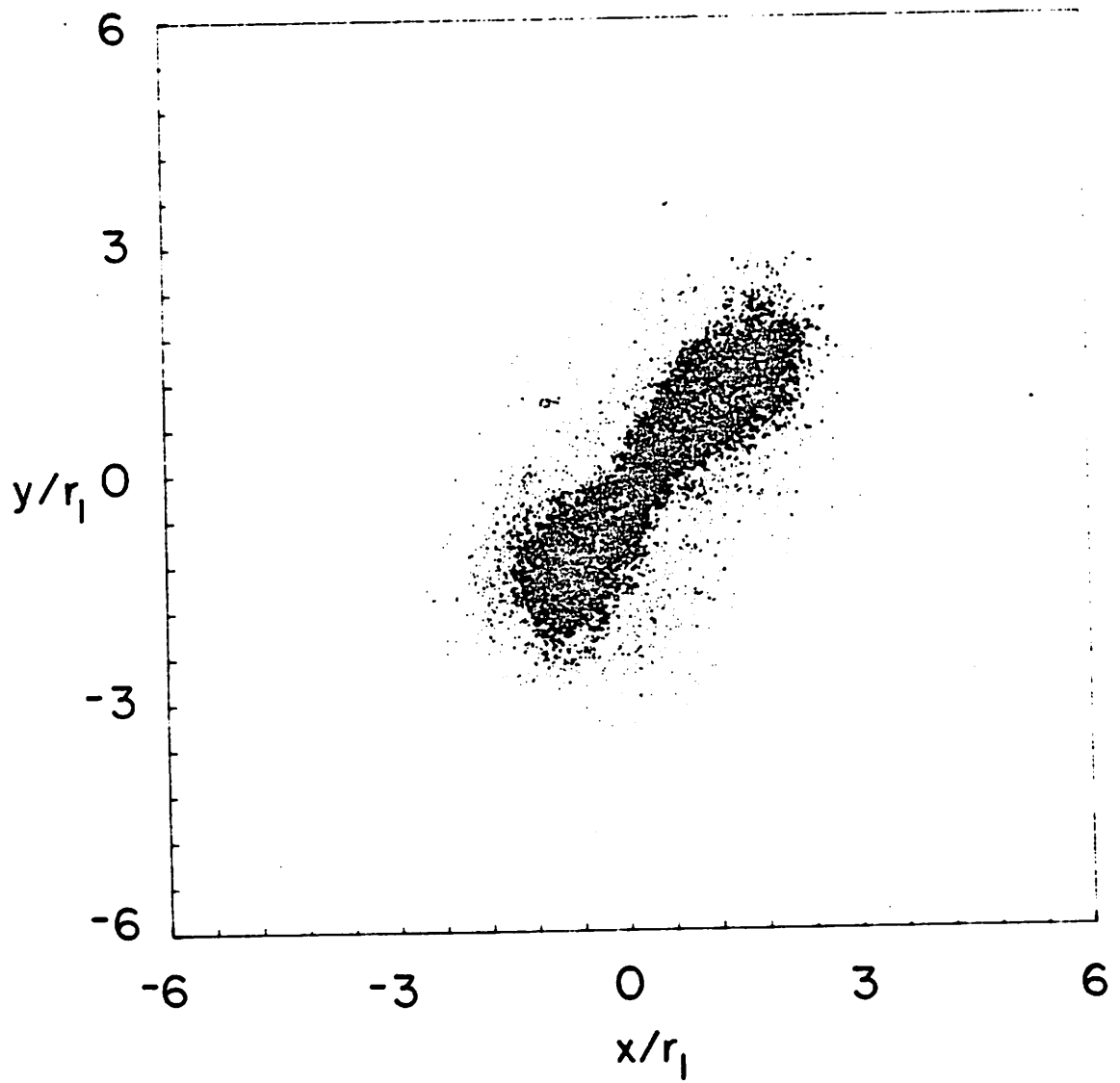


FIG. 6d.

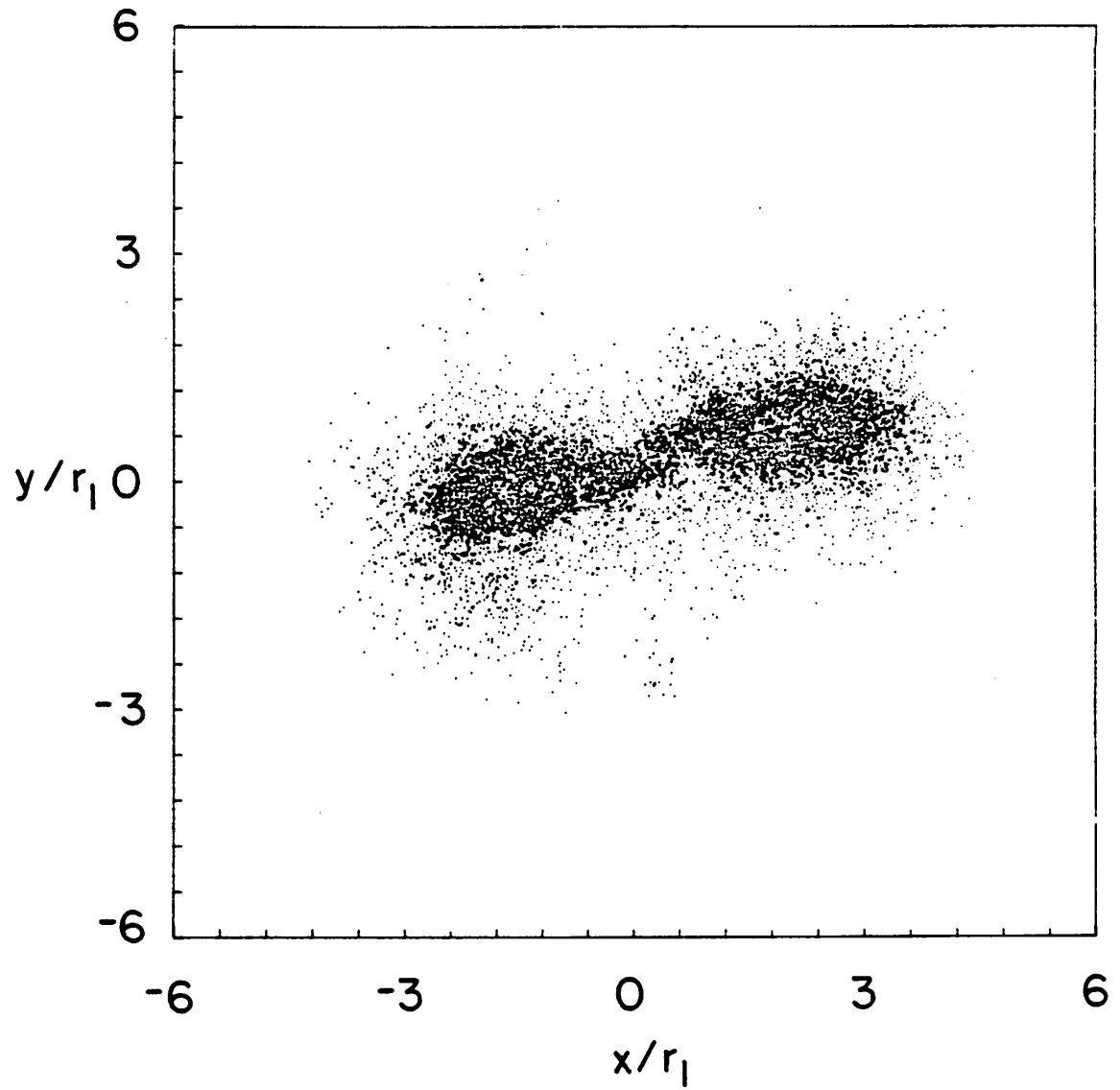


FIG. 6e.

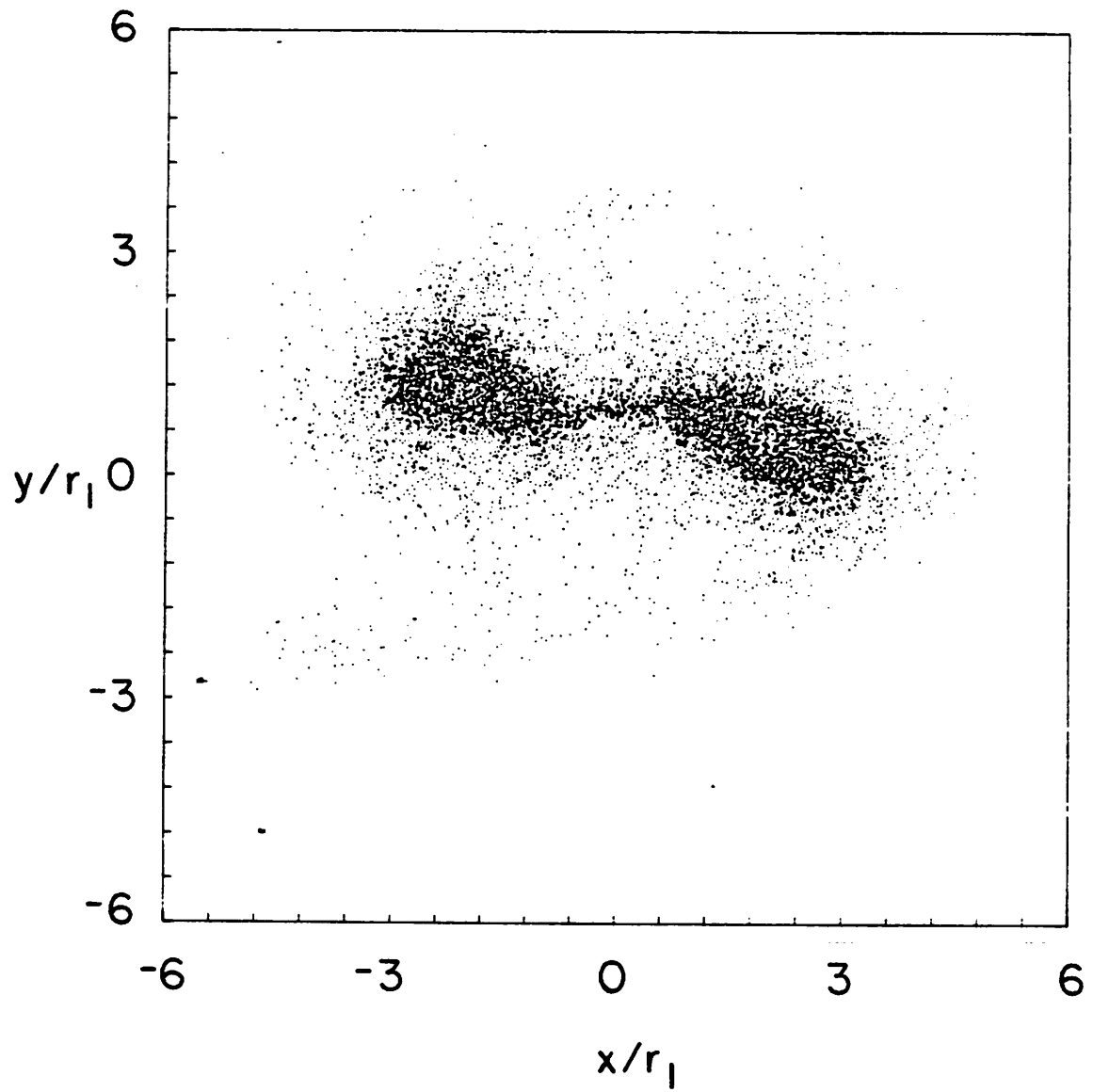


FIG. 6f.

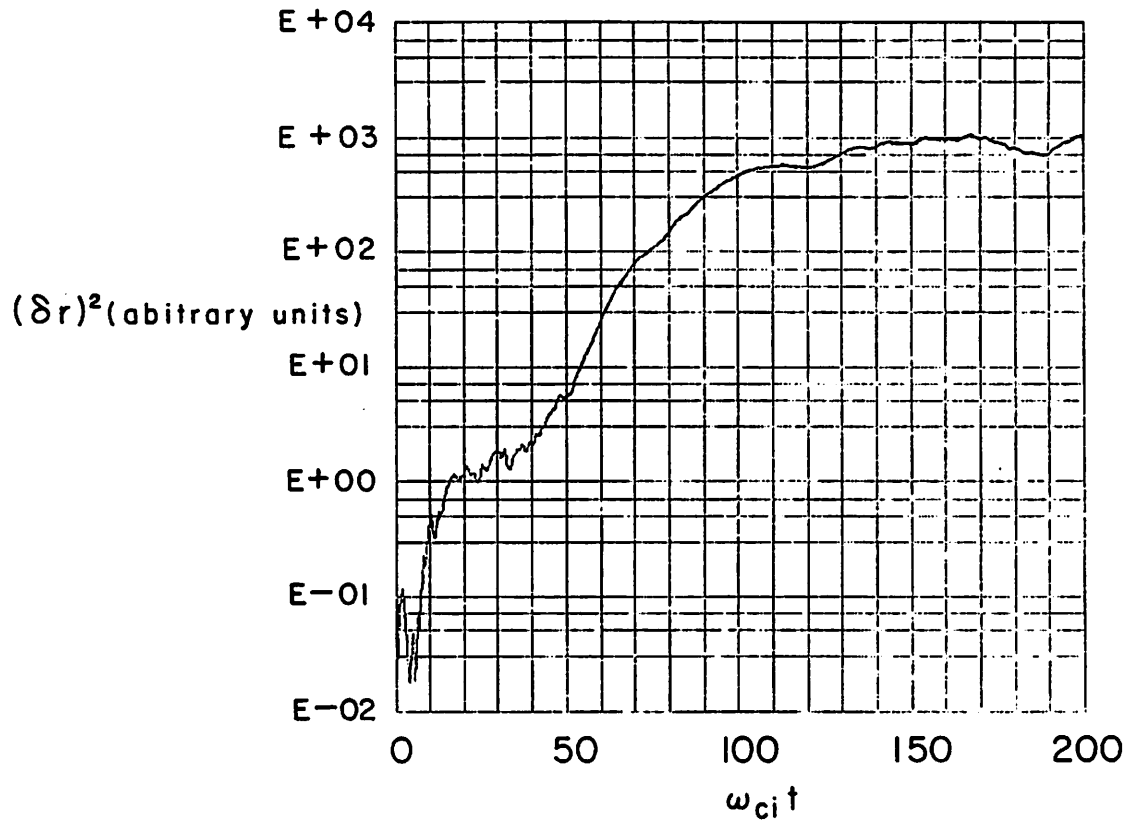


FIG. 7. $(\delta r)^2$ for mode 2 as a function of time for the simulation run of Fig. 6.

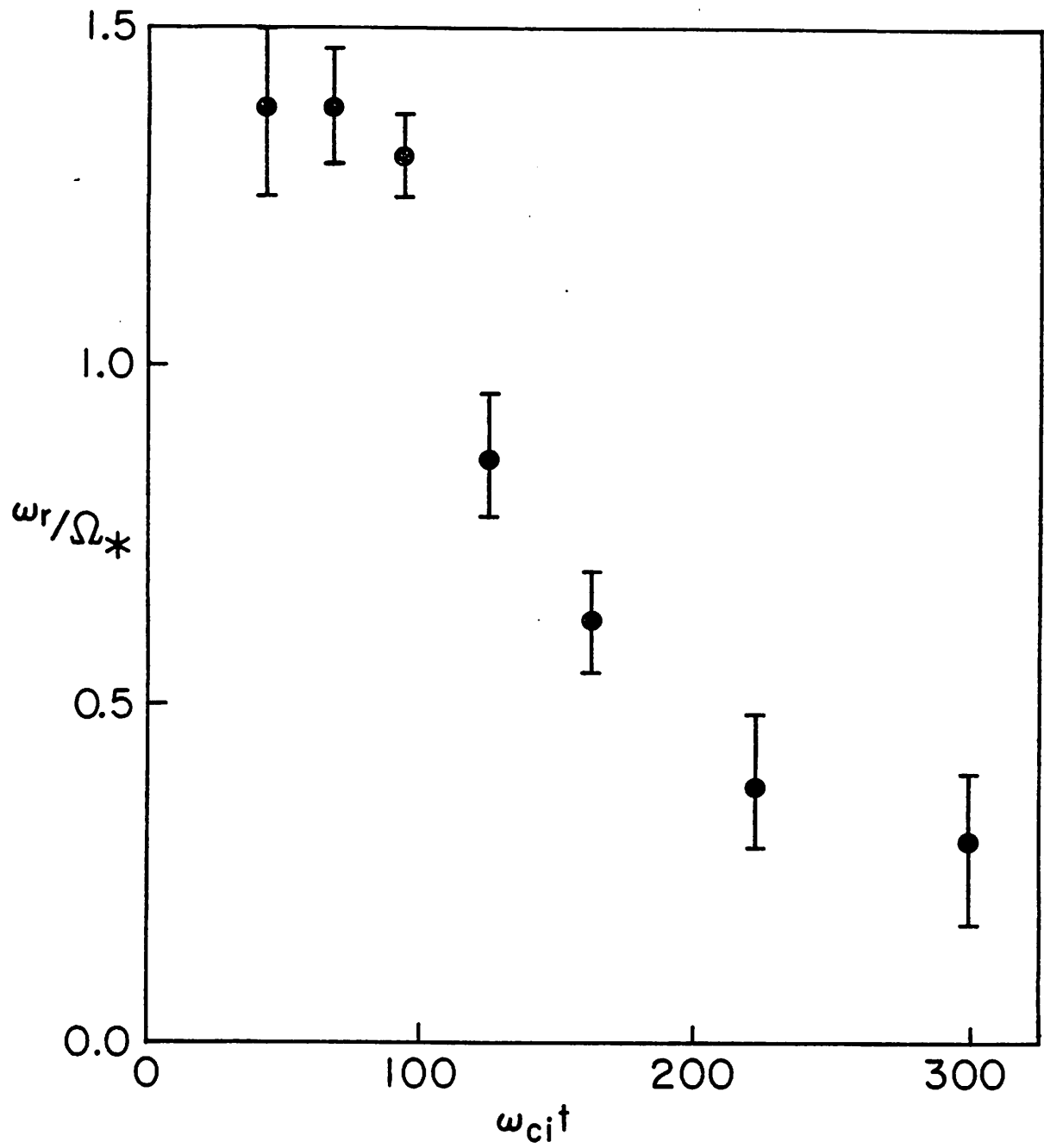


FIG. 8. Real frequencies, ω_r , as a function of time for the simulation run of Fig. 6.

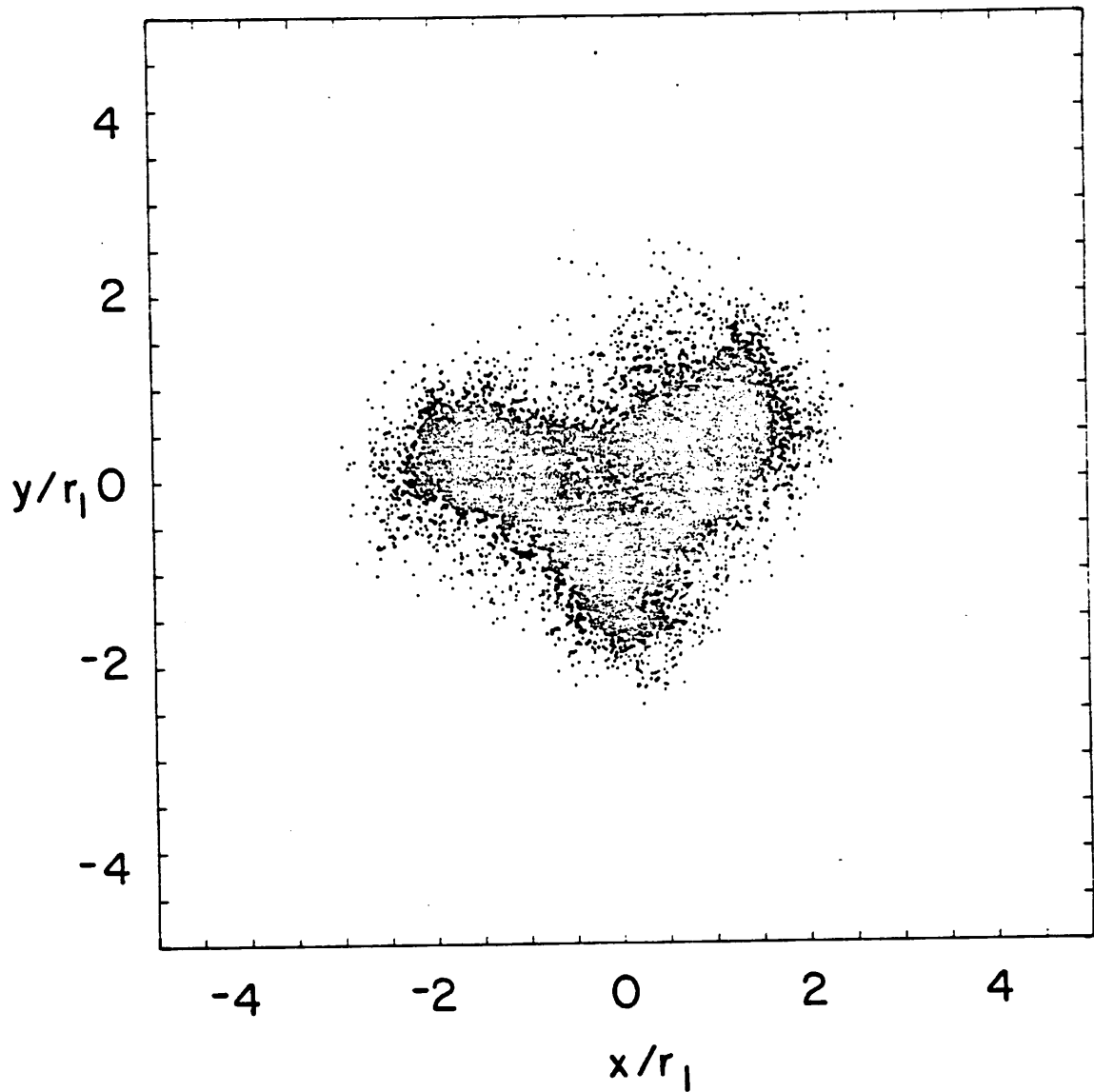


FIG. 9. Particle positions in the r - θ plane at $t=110\omega_{ci}^{-1}$. $\Omega_+ = 0.05\omega_{ci}$, $\beta_0 = 0.23$, and $\alpha = 1.0$.